RSC Advances

PAPER

View Article Online
View Journal | View Issue

Cite this: *RSC Adv.*, 2019, **9**, 27937

A novel ratiometric AIEE/ESIPT probe for palladium species detection with ultra-sensitivity†

Zixuan Xu,[a] Mingshu Zhang,[a] Rui Zhang,[a] Shudi Liu[b] and Ying Yang *[a]

Received 4th August 2019
Accepted 22nd August 2019

DOI: 10.1039/c9ra06046d

rsc.li/rsc-advances

Existing fluorescent probes for palladium (Pd) species detection have revealed their vulnerabilities, such as low sensitivity, poor anti-interference ability and long reaction time. In order to develop a faster and more accurate detection method for palladium species at extremely low concentrations, in this study, we designed a novel ratiometric AIEE/ESIPT probe (**HPNI-1**) based on the Tsuji–Trost reaction for Pd. According to the data obtained, the probe was able to detect Pd species with an ultra-high anti-interference ability (Pd : other metals = 1 : 1000), rapid detection time (within 2 minute) and ratiometric fluorescent signal changes with a 1.34 nM detection limit. This study not only proves that existing methods can be improved but also provides future prospects for **HPNI-1** as one of the greatest probes for Pd species detection.

1. Introduction

Palladium (Pd) plays a crucial role in various fields, such as functional materials, electric equipment, automobile exhaust catalysts, jewelry, and chemical transformations.[1–5] However, due to limited Pd resources and extractive technologies, the supply is not able to meet the demand, causing difficulties in actual applications. Moreover, the environmental pollution caused by the frequent use of Pd hinders the aim of sustainable development. Moreover, according to some meaningful studies, easily forming complexes between Pd and some bio-macromolecules, such as proteins, DNA and RNA, have the possibility of causing serious health problems.[6,7] The European Agency for the Evaluation of Medicinal Products (EMEA) suggested that the threshold for residual Pd is 5–10 ppm.[8] Hence, it is critical to develop efficient methods for detecting Pd species.

Traditional detection methods for palladium species, include X-ray fluorescence, atomic absorption spectrometry (AAS), and solid phase microextraction-high performance liquid chromatography.[9,10] However, these methods require expensive instruments and high-level technicians. Recently, fluorescence detection for Pd has been a focal area owing to its high sensitivity, high selectivity, simple operation and cost-effectiveness.[11]

Currently, fluorescent probes for palladium species detection are mainly based on coordination and catalytic mechanisms. However, the majority of the coordination mechanism-based probes show poor anti-interference ability relative to other transition metal ions.[12] On the contrary, probes based on a catalytic mechanism usually show superior selectivity.[13–20] However, we noticed that some limitations still exist in the detection of palladium based on catalytic mechanism, such as long detection times and detection difficulty in extremely low concentrations.[21–25] In addition, most fluorophores of fluorescence probes exhibit relatively small Stokes shifts, which hinders their applications in quantitative determination due to self-absorption.[18,26–28] Moreover, many probes detect OFF–ON or ON–OFF signal output changes in their fluorescence intensity. This type of probe with a single fluorescence change could be significantly influenced by environmental effects, along with a decrease in signal fidelity.[24,29,30] Therefore, we urgently need to develop a palladium fluorescent probe that can overcome the difficulties described above.[31,32]

Thus, we present a novel ratiometric probe **HPNI-1** for palladium species based on aggregated induced enhanced emission (AIEE) and excited-state intramolecular proton transfer (ESIPT) mechanisms (Fig. S2 and S3†). We specifically selected HPNI as the AIEE fluorophore, and the terminal allyl chloroformate was used as the recognition site and was modified on the hydroxyl group of HPNI to block the ESIPT process.[33] After palladium treatment, the ESIPT process was recovered under ultraviolet excitation, resulting in tautomerization and a large Stokes shift (240 nm) (shown in Schemes 2 and 3). Moreover, we were able to get a meaningful data that showed that **HPNI-1** had an ultra-fast reaction time and ultra-low detection concentration for palladium detection. Thus, we suggest that **HPNI-1** is one of the best fluorescent probes of palladium species detection.

[a]*Laboratory of Nonferrous Metals Chemistry and Resources Utilization of Gansu Province, College of Chemistry and Chemical Engineering, Lanzhou University, Lanzhou 730000, Gansu, P. R. China. E-mail: yangying@lzu.edu.cn*

[b]*College of Chemistry and Chemical Engineering, Yantai University, Yantai, 264005, P. R. China*

† Electronic supplementary information (ESI) available: Materials and methods, synthesis, the characterization data of **HPNI-1** and additional spectra. See DOI: 10.1039/c9ra06046d

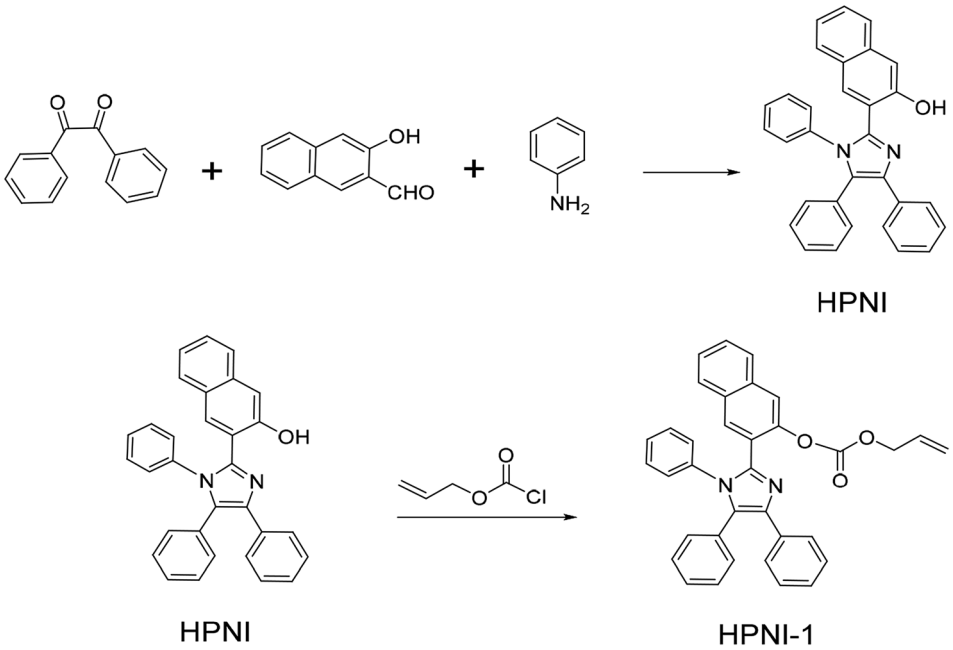

Scheme 1 Synthesis of HPNI-1.

2. Material and methods

2.1 Materials and instruments

All reagents and solvents were obtained commercially and used without further purification unless otherwise noted. ^{1}H NMR and ^{13}C NMR spectra were recorded on a JEOLBCS 400M spectrometer. Mass spectra (ESI) were recorded on a LQC system (Finnigan MAT, USA). All UV-visible spectra were recorded on a Varian Cary 100 spectrophotometer. Fluorescence spectra were recorded using an Edinburgh FLSP920. Fluorescence spectra were recorded after the addition of palladium for 1 min.

2.2 Synthesis of HPNI and HPNI-1

Precursor HPNI was prepared according to the following procedures.[9]

To a solution of HPNI (200 mg, 0.456 mmol) and allyl chloroformate (0.5 mL) in THF (20 mL), was added triethylamine (0.15 mL, 1 mmol) dropwise at 0 °C for 30 min. After that, the mixture was stirred at room temperature for 2 h. Then, the mixture was extracted with dichloromethane, and the combined organic phase was dried over anhydrous Na_2SO_4. The solvent was removed under reduced pressure, and the residue was purified *via* column chromatography on silica gel with a mixture of ethyl acetate/petroleum ether (1 : 4, v/v) as the eluent to obtain **HPNI-1** as a yellow solid (0.21 g, 90.3%). ^{1}H NMR (400 MHz, $CDCl_3$) δ 7.69 (d, J = 8.1 Hz, 1H), 7.65 (s, 1H), 7.60 (s, 1H), 7.53 (d, J = 7.1 Hz, 3H), 7.37 (ddd, J = 29.2, 11.0, 4.0 Hz, 2H), 7.23–7.14 (m, 5H), 7.14–7.03 (m, 6H), 6.98 (dd, J = 8.0, 1.5 Hz, 2H), 5.73 (ddt, J = 16.3, 10.5, 5.8 Hz, 1H), 5.12 (ddd, J = 13.8, 11.5, 1.2 Hz, 2H), 4.52 (d, J = 5.8 Hz, 2H). ^{13}C NMR (101 MHz, $CDCl_3$) δ 153.04, 146.72, 142.94, 138.46, 136.63, 134.43, 133.49, 132.19, 131.18, 131.13, 130.82, 130.67, 130.51, 128.81, 128.42, 128.08, 128.00, 127.43, 127.30, 126.59, 126.19, 119.56, 119.21, 69.18. ESI-MS: calcd for [$C_{35}H_{26}N_2O_3$ + H^+], 523.2016; found, 523.2028.

2.3 General procedure for spectral measurements

HPNI-1 (1 mM) was dissolved in THF and maintained at room temperature. Stock solutions of $Pd(PPh_3)_4$, $Pd(PPh_3)_2Cl_2$, $Pd_2(dba)_3$, and $(C_3H_5)_2PdCl_2$ (0.1 mM) were prepared in DMSO as the sources of Pd and used freshly. Zn^{2+}, Ni^{2+}, Na^{2+}, Mn^{2+}, K^+, Cr^{3+}, Co^{2+}, Cd^{2+}, Ca^{2+}, Ba^{2+}, NO^{3-}, Cl^-, SO_4^{2-}, CO_3^{2-}, AcO^-, SCN, and I^- (10 mM) were prepared in deionized water by dissolving the corresponding salts. Test solutions were prepared by placing 20 μL of **HPNI-1** stock solution into a quartz cell, diluting the solution to 2 mL with an acetonitrile-and-water mixed solution ($CH_3CN : H_2O$ = 3 : 2, KBH_4 = 1 mM), and then different analytes were added. All of the UV-vis absorption and fluorescence measurements were taken at room temperature. The selected excitation and emission wavelengths were at

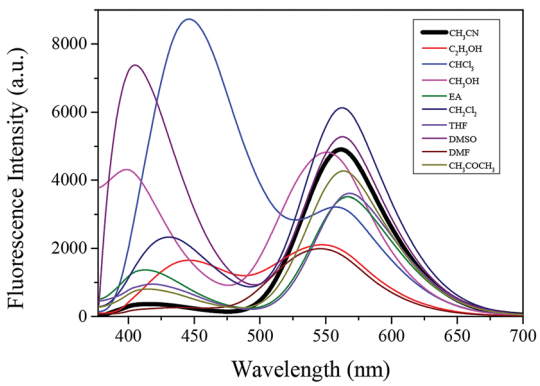

Fig. 1 Emission spectra of HPNI in different solutions. Concentration 10 μM, λ_{ex} = 365 nm.

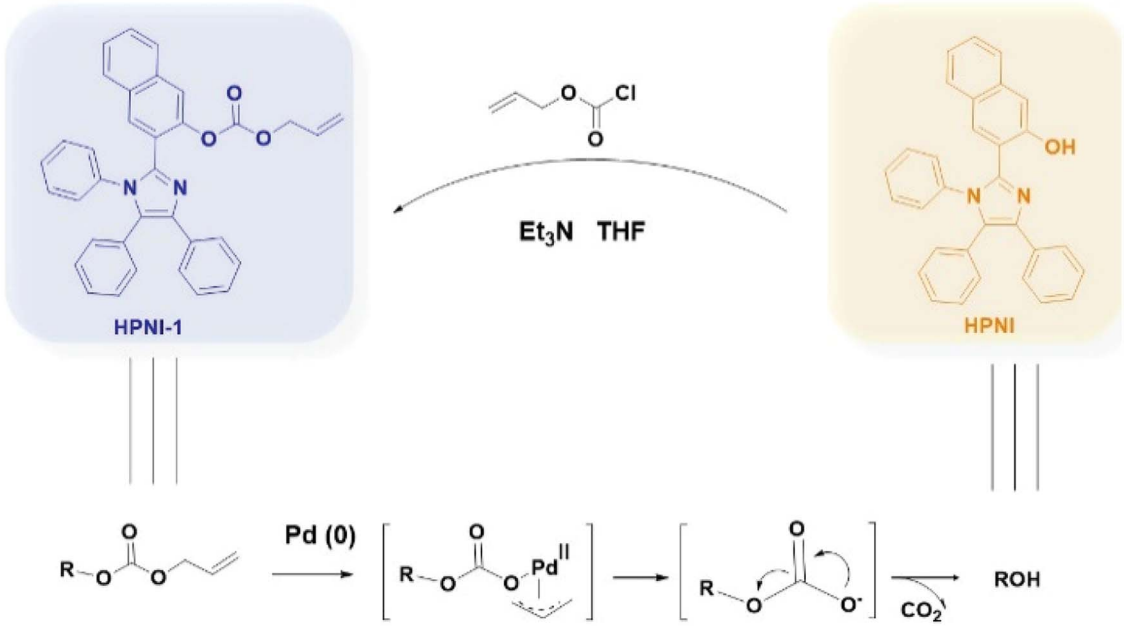

Scheme 2 The sensing mechanism of **HPNI-1** for the selective recognition of palladium.

365 nm and 570 nm, respectively. The excitation slit width was 5 nm, and emission slit width was 5 nm. The fluorescence spectra were recorded after 2 min after the addition of analytes into the quartz cell to allow the complete mixing of the analytes into the solution.

2.4 Determination of the detection limit

According to the fluorescence titration, the fluorescence intensity ratio (I_{570}/I_{410}) and the concentration of Pd(0) (0–50 nM) showed an excellent linear relationship. The detection limit was calculated by the following equation:

$$\text{Detection limit} = 3\sigma/k \quad (1)$$

where σ is the standard deviation of the blank sample (measured 10 times) and k is the slope of the linear regression equation.

3. Results and discussion

The synthetic process of the probe **HPNI-1** is shown in Scheme 1. We chose HPNI as the fluorophore due to its large Stokes shift (240 nm) by the excited-state intramolecular proton transfer (ESIPT) process. This fluorophore also has a high fluorescence quantum yield (Φ = 0.22). Terminal allyl chloroformate was used as the recognition site, which was modified on the hydroxyl group of HPNI to block the ESIPT process. **HPNI-1** was characterized by ^{1}H NMR, ^{13}C NMR and HR-MS.

3.1 The fluorescence spectrum of HPNI in various solutions

The emission spectra of HPNI in different solutions are shown in Fig. 1. We noticed that HPNI has dual emission bands, which can be attributed to the coexistence of two tautomers in the ESIPT process (Scheme 3). We suggest that the shorter emission bands are ascribed to the enol form of HPNI. Relatively, the

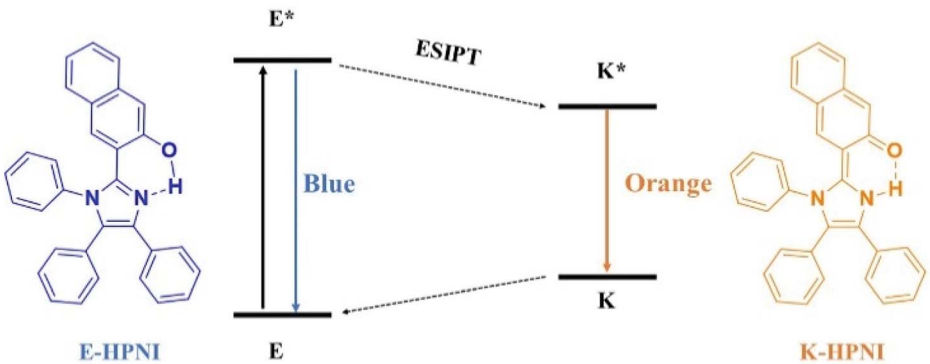

Scheme 3 General mechanism of ESIPT process and chemical structures of enol form (E) and keto from (K) in the ESIPT process of HPNI.

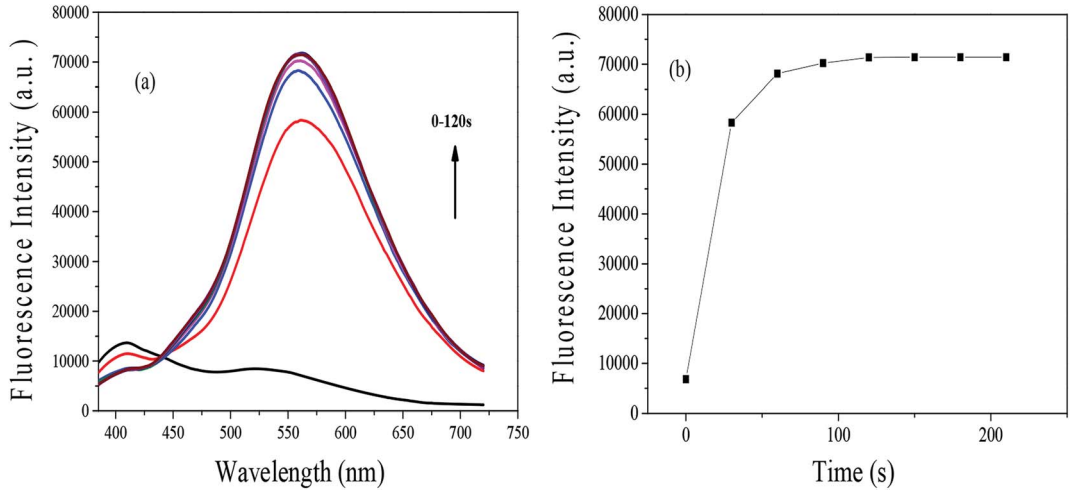

Fig. 2 (a) Fluorescence spectral changes of **HPNI-1** (10 μM) and (b) the relationship between fluorescence intensity and reaction time upon treatment with $Pd(PPh_3)_4$ (2 μM) in acetonitrile–water solution ($CH_3CN : H_2O = 3 : 2$, KBH_4 (1 mmol)) Ex = 365 nm.

longer emission band can be assigned to the keto form of HPNI. HPNI exhibits strong fluorescence emission at 570 nm and extremely weak fluorescence emission at 410 nm in acetonitrile, indicating that the keto form is the main form of HPNI in acetonitrile. Therefore, choosing acetonitrile as the solvent makes detection more reliable. In addition, in the mixed solution of CH_3CN and H_2O at various ratios, HPNI and **HPNI-1** had relatively high fluorescence intensities when $CH_3CN : H_2O = 3 : 2$ (Fig. S1 and S2†). Therefore, we chose $CH_3CN : H_2O = 3 : 2$ mixed solutions as a solvent.

3.2 Fluorescence response toward Pd(0)

The fluorescence spectra of **HPNI-1** ($CH_3CN : H_2O = 3 : 2$, KBH_4: 1 mmol) at room temperature was investigated (Fig. 2), and **HPNI-1** showed fluorescence emission at 410 nm upon excitation at 365 nm. After reaction with palladium, a decrease in the emission intensity at 410 nm was observed. Moreover, a new emission band appeared at 570 nm, which created an isosbestic point at 460 nm that exhibited a ratiometric response. The large red-shift (160 nm) is due to the ESIPT process being recovered. Notably, the fluorescence intensity reached equilibrium within 2 min.

3.3 The sensitivity

Fig. 3a shows the fluorescence changes with various amounts of $Pd(PPh_3)_4$ in a $CH_3CN : H_2O$ (3 : 2 v/v) solution with KBH_4 (1 mM) after 2 min. When the concentration of $Pd(PPh_3)_4$ gradually increases, the fluorescence peak at $\lambda = 410$ nm shows a slow decrease, and a new fluorescence peak appears at $\lambda = 570$ nm and then becomes the maximum peak. The ratio of the fluorescence intensities ($\lambda_{570}/\lambda_{410}$) changes from 0.18 to 5.34 (R = 30.24-fold). More importantly, as the concentration of $Pd(PPh_3)_4$ increases from 0 to 500 nM, the ratio of the fluorescent intensity shows an excellent linear relationship.

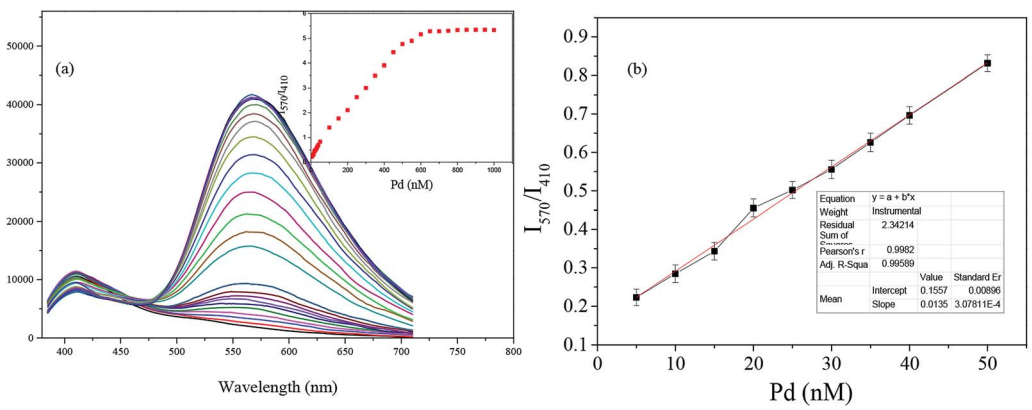

Fig. 3 (a) Fluorescent spectral changes of **HPNI-1** (10 μM) upon addition of different concentrations of $Pd(PPh_3)_4$ (0–1 μM) in acetonitrile–water solutions ($CH_3CN : H_2O = 3 : 2$, KBH_4: 1 mM) at room temperature. Each spectrum was obtained 2 min after $Pd(PPh_3)_4$ addition. Ex = 365 nm. Slit: 5.0 nm/5.0 nm. Inset: The fluorescent intensity ratio changes at 570 and 410 nm (I_{570}/I_{410}) against the concentrations of $Pd(PPh_3)_4$. (b) Linear relationship of the I_{570}/I_{410} as a function of the concentration of $Pd(PPh_3)_4$ from 5 to 50 nM.

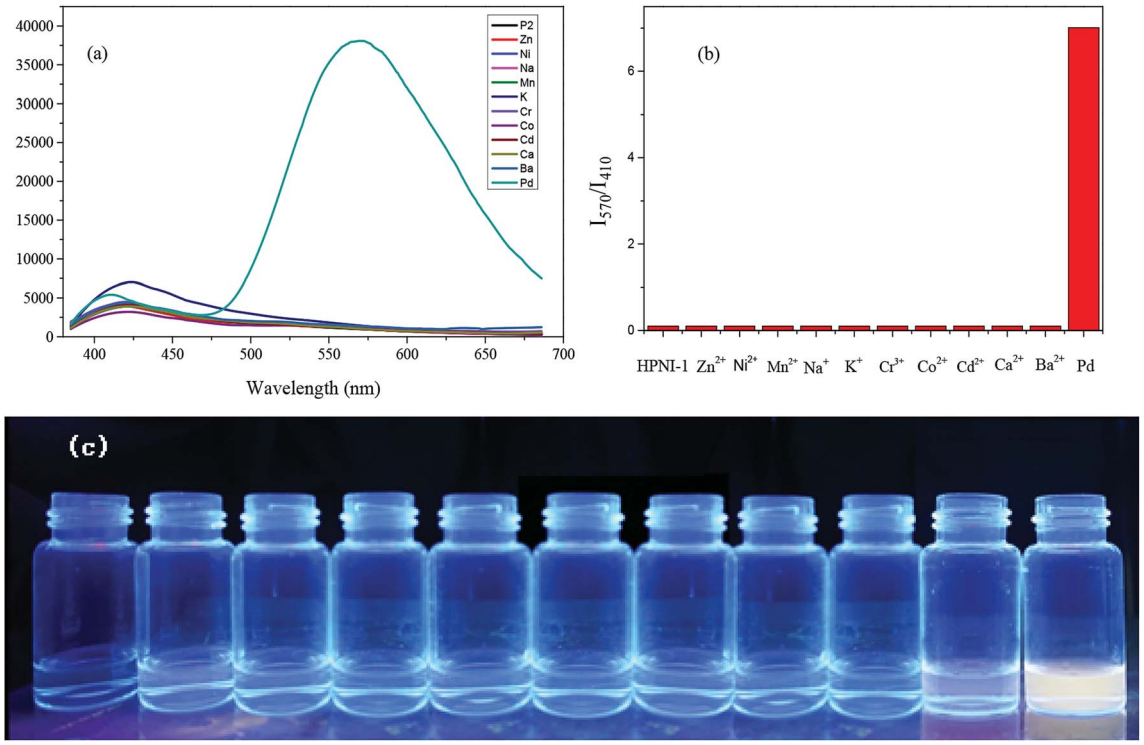

Fig. 4 (a) Fluorescent spectral (b) fluorescence intensity and (c) photograph of **HPNI-1** (10 μM) with the addition of $Pd(PPh_3)_4$ (1 μM) and other metal ions (1 mM) in acetonitrile–water solutions (CH_3CN : H_2O = 3 : 2, KBH_4: 1 mM) at room temperature. Each spectrum was obtained 2 min after the metal ion addition. Ex = 365 nm. Slit: 5.0 nm/5.0 nm.

The ratiometric fluorescent detection method is based on the ratio of the two fluorescent bands rather than the absolute emission intensity of one band, making it possible to analyze palladium species more accurately and sensitively by minimizing the background signal. Moreover, under the ultra-low concentrations of $Pd(PPh_3)_4$, the good linear relationship is maintained (Fig. 3b). According to the data presented in the research and eqn (1), the detection limit of **HPNI-1** for Pd(0) is 1.34 nM. (The sensitivity of **HPNI-1** was far beyond those of other reported studies and much lower than the palladium content in the samples of human saliva (7.4 μg L^{-1})). That is, **HPNI-1** can serve as a sensitive ratiometric fluorescent sensor for the quantitative detection of Pd.

3.4 The sensitivity

Selectivity experiments were performed with different metal ions (Fig. 4). In the mixed solution (CH_3CN : H_2O = 3 : 2, KBH_4 = 1 mM), the ratiometric response can only be detected when Pd(0) (1 μM) is added to the solution. Other metals such as Zn^{2+}, Ni^{2+}, Na^{2+}, Mn^{2+}, K^{+}, Cr^{3+}, Co^{2+}, Cd^{2+}, Ca^{2+} and Ba^{2+} (1 mM) have no or an insignificant influence on the detection. Under UV light (365 nm), significant orange fluorescence is observed. The

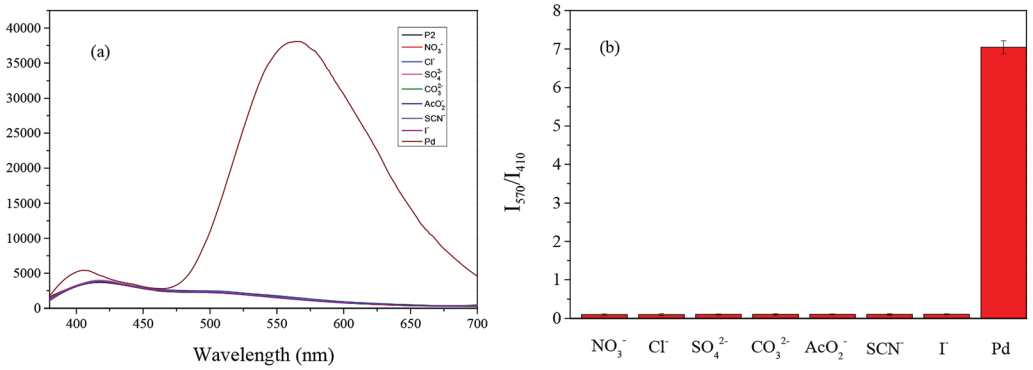

Fig. 5 (a) Fluorescence spectra and (b) fluorescence intensity of **HPNI-1** (10 μM) with the addition of $Pd(PPh_3)_4$ (1 μM) and other anions (1 mM) in acetonitrile–water solutions (CH_3CN : H_2O = 3 : 2, KBH_4: 1 mM) at room temperature. Each spectrum was obtained 2 min after metal ion addition. Ex = 365 nm. Slit: 5.0 nm/5.0 nm.

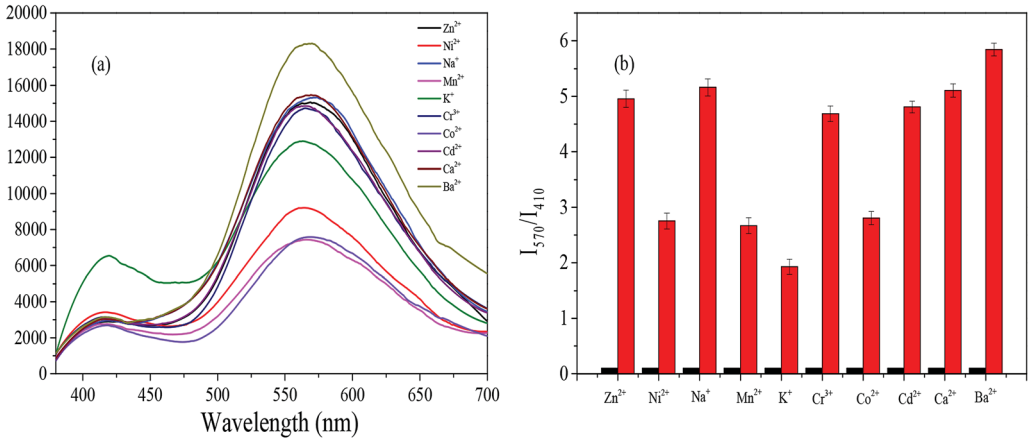

Fig. 6 (a) Fluorescence detection and (b) fluorescence intensity ratio (I_{570}/I_{410}) of $Pd(PPh_3)_4$ (0.3 μM) with **HPNI-1** (10 μM) in the presence of other metal ions (0.3 mM) in acetonitrile–water solutions (CH_3CN : H_2O = 3 : 2, KBH_4: 1 mM) at room temperature. Each spectrum was obtained 2 min after metal ion addition. Ex = 365 nm. Slit: 5.0 nm/5.0 nm.

experimental results of the interference of the above-mentioned metal ions on Pd(0) show that **HPNI-1** possesses ultra-high selectivity for palladium detection. ($[Pd(0)]/[M^{n+}] = 1 : 1000$).

Similarly, we conducted selectivity and anti-interference experiments on the anions (NO^{3-}, Cl^-, SO_4^{2-}, CO_3^{2-}, AcO^-, SCN, and I^-) (Fig. 5), and **HPNI-1** again showed excellent selectivity for the palladium species.

3.5 The anti-interference ability

We also investigated the anti-interference ability of **HPNI-1**; as shown in Fig. 6, we can observe the fluorescence responses for Pd(0) detection at high concentrations of the metal ion solutions (metal ions : $Pd(PPh_3)_4$ = 1000 : 1). Due to its ultra-high anti-interference characteristic, **HPNI-1** possesses a great practical application value for Pd(0) detection.

3.6 The sensing behavior of HPNI-1 for other palladium sources

To verify the potential application of **HPNI-1**, we tested whether the probe could detect all the oxidation states of Pd [Pd(0) : $Pd(PPh_3)_4$, $Pd_2(dba)_3$; Pd(II) : $PdCl_2(PPh_3)_2$, $(C_3H_5)_2PdCl_2$; Pd(IV) : K_2PdCl_6]. According to the intensity ratio (I_{570}/I_{410}), the sensitivity of **HPNI-1** to palladium was $PdCl_2(PPh_3)_2$ > $Pd(PPh_3)_4$ > $Pd_2(dba)_3$ > $(C_3H_5)_2PdCl_2$ > K_2PdCl_6, as shown in Fig. 7. The results showed that **HPNI-1** has a significant response to all the oxidation states of palladium, and the fluorescence changed significantly. In addition, we noticed that in the detection of palladium complexes, containing organic ligands had relatively stronger fluorescence intensities.

To deeply investigate the reaction mechanism of **HPNI-1** and $Pd(PPh_3)_4$, ^1H NMR titration experiment was performed in

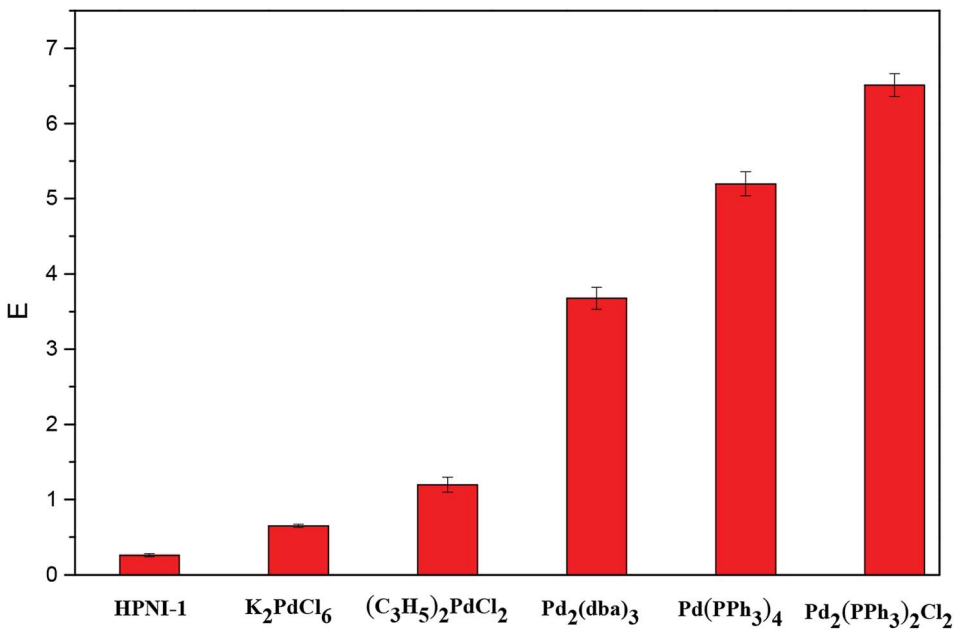

Fig. 7 The fluorescence responses of **HPNI-1** (10 μM) to various palladium sources (1 μM). (CH_3CN : H_2O = 3 : 2, KBH_4: 1 mM).

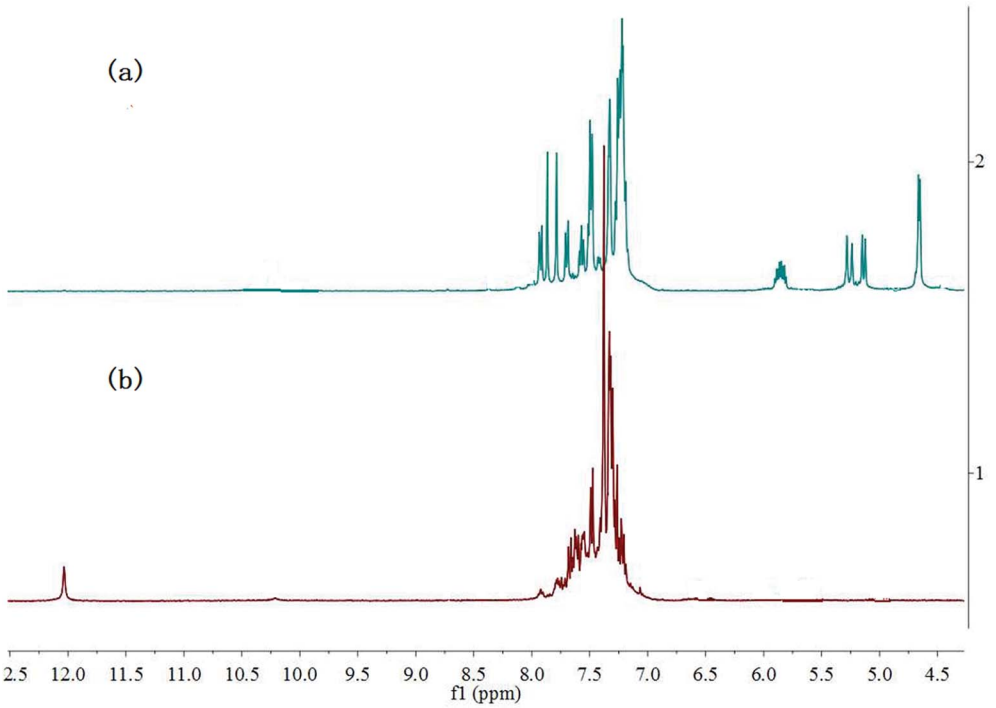

Fig. 8 Stacked ^{1}H NMR spectra of (a) **HPNI-1** and (b) upon addition of $Pd(PPh_3)_4$ in DMSO-d_6.

DMSO-d_6 (Fig. 8). For **HPNI-1**, the multiple peaks between 5.75 and 5.93 ppm and the doublet peaks appearing at 5.28 and 5.15 ppm were assigned to the CH═ and ═CH_2 protons in the allyl group, respectively (Fig. 8a). These characteristic peaks disappeared in the ^{1}H NMR spectrum after $Pd(PPh_3)_4$, treatment (0.1 equiv.) (Fig. 8b). Moreover, a new peak attributed to the OH group in HPNI appeared at 12.03 ppm. It is clear that the ^{1}H NMR spectrum is almost identical to that of standard HPNI,[33] demonstrating that the reaction of **HPNI-1** with Pd^0 results in the release of HPNI–OH. Based on these results and some previous reports, the mechanism of **HPNI-1** for Pd^0 detection is illustrated in Scheme 2.

4. Conclusion

In conclusion, we successfully synthesized a novel fluorescence probe (**HPNI-1**) for palladium species detection based on a Pd(0)-triggered cleavage reaction. **HPNI-1** possessed ultra-high selectivity and anti-interference ability. Moreover, **HPNI-1** exhibited obvious ratiometric fluorescence responses toward palladium due to the ESIPT process, with a color change from weak blue to strong orange. Moreover, the probe had an astonishing detection limit (1.34 nM), which has far exceeds those of other reported probes. Thus, we suggest that **HPNI-1** has great potential to detect ultra-low concentrations of palladium species in environmental settings.

Conflicts of interest

The authors declare no competing financial interest.

Acknowledgements

This work was supported by the National Natural Science Foundation of China (Grant 51474118, 21701074).

References

1 SESSION, DWHORATR International Programme on Chemical Safety, 2009.
2 R. Martin and S. L. Buchwald, *Acc. Chem. Res.*, 2008, **41**, 1461–1473.
3 W. Wu and H. Jiang, *Acc. Chem. Res.*, 2012, **45**, 1736–1748.
4 S.-Y. Ding, J. Gao, Q. Wang, Y. Zhang, W.-G. Song, C.-Y. Su and W. Wang, *J. Am. Chem. Soc.*, 2011, **133**, 19816–19822.
5 Z. He, B. Dong, W. Wang, G. Yang, Y. Cao, H. Wang, Y. Yang, Q. Wang, F. Peng and H. Yu, *ACS Catal.*, 2019, **9**, 2893–2901.
6 J. Wataha and C. Hanks, *J. Oral Rehabil.*, 1996, **23**, 309–320.
7 J. Kielhorn, C. Melber, D. Keller and I. Mangelsdorf, *Int. J. Hyg. Environ. Health*, 2002, **205**, 417–432.
8 C. E. Garrett and K. Prasad, *Adv. Synth. Catal.*, 2004, **346**, 889–900.
9 K. Van Meel, A. Smekens, M. Behets, P. Kazandjian and R. Van Grieken, *Anal. Chem.*, 2007, **79**, 6383–6389.
10 C. Locatelli, D. Melucci and G. Torsi, *Anal. Bioanal. Chem.*, 2005, **382**, 1567–1573.
11 H. Li, J. Fan and X. Peng, *Chem. Soc. Rev.*, 2013, **42**, 7943–7962.
12 M. N. Yaraşir, M. Kandaz, A. Koca and B. Salih, *Polyhedron*, 2007, **26**, 1139–1147.
13 J. Jiang, H. Jiang, W. Liu, X. Tang, X. Zhou, W. Liu and R. Liu, *Org. Lett.*, 2011, **13**, 4922–4925.

14 M. Santra, S.-K. Ko, I. Shin and K. H. Ahn, *Chem. Commun.*, 2010, **46**, 3964–3966.
15 B. Liu, H. Wang, T. Wang, Y. Bao, F. Du, J. Tian, Q. Li and R. Bai, *Chem. Commun.*, 2012, **48**, 2867–2869.
16 R. M. Yusop, A. Unciti-Broceta, E. M. Johansson, R. M. Sánchez-Martín and M. Bradley, *Nat. Chem.*, 2011, **3**, 239.
17 Q. Xia, S. Feng, D. Liu and G. Feng, *Sens. Actuators, B*, 2018, **258**, 98–104.
18 W. Feng, L. Bai, S. Jia and G. Feng, *Sens. Actuators, B*, 2018, **260**, 554–562.
19 X. Jie, M. Liu, A. Peng, J. Huang, Y. Zhang, X. Wang and Z. Tian, *Talanta*, 2018, **183**, 164–171.
20 J. Zhou, S. Xu, Z. Yu, X. Ye, X. Dong and W. Zhao, *Dyes Pigm.*, 2019, **170**, 107656.
21 W. Luo, J. Li and W. Liu, *Org. Biomol. Chem.*, 2017, **15**, 5846–5850.
22 B. Zhu, C. Gao, Y. Zhao, C. Liu, Y. Li, Q. Wei, Z. Ma, B. Du and X. Zhang, *Chem. Commun.*, 2011, **47**, 8656–8658.
23 H. Chen, W. Lin and L. Yuan, *Org. Biomol. Chem.*, 2013, **11**, 1938–1941.
24 J.-w. Yan, X.-l. Wang, Q.-f. Tan, P.-f. Yao, J.-h. Tan and L. Zhang, *Analyst*, 2016, **141**, 2376–2379.
25 T. Gao, P. Xu, M. Liu, A. Bi, P. Hu, B. Ye, W. Wang and W. Zeng, *Chem.–Asian J.*, 2015, **10**, 1142–1145.
26 X. Teng, M. Tian, J. Zhang, L. Tang and J. Xin, *Tetrahedron Lett.*, 2018, **59**, 2804–2808.
27 H. Nie, J. Geng, J. Jing, Y. Li, W. Yang and X. Zhang, *RSC Adv.*, 2015, **5**, 97121–97126.
28 W. Luo and W. Liu, *Dalton Trans.*, 2016, **45**, 11682–11687.
29 M. Liu, T. Leng, K. Wang, Y. Shen and C. Wang, *J. Photochem. Photobiol., A*, 2017, **337**, 25–32.
30 W. Su, B. Gu, X. Hu, X. Duan, Y. Zhang, H. Li and S. Yao, *Dyes Pigm.*, 2017, **137**, 293–298.
31 L. Zhou, Q. Wang, X.-B. Zhang and W. Tan, *Anal. Chem.*, 2015, **87**, 4503–4507.
32 L. Zhou, S. Hu, H. Wang, H. Sun and X. Zhang, *Spectrochim. Acta, Part A*, 2016, **166**, 25–30.
33 S. Park, J. E. Kwon, S. H. Kim, J. Seo, K. Chung, S.-Y. Park, D.-J. Jang, B. M. Medina, J. Gierschner and S. Y. Park, *J. Am. Chem. Soc.*, 2009, **131**, 14043–14049.